

FOCUSING CHARACTERISTICS OF A METALLIC CYLINDRICAL ELECTROMAGNETIC BAND GAP STRUCTURE WITH DEFECTS

H. Boutayeb, A.-C. Tarot, and K. Mahdjoubi

IETR, UMR 6164 CNRS
University of Rennes
Ave. Général Leclerc 35042 Rennes Cedex, France

Abstract—The focusing characteristics of 2D-Cylindrical Electromagnetic Band Gap (CEBG) structures constituted of metallic wires and with defects are analyzed numerically for directive antennas application. The introduction of defects into the periodic structures consists of removing one or multiple wires. The simulations were carried out with a Finite Difference Time Domain (FDTD) code, where the excitation is a line source and the CEBG structure is considered infinite in the vertical direction. Numerical results showing the effects of the number of cylindrical layers and of the number of defects are presented and discussed. These results allow to determine the structures giving best focusing performance and to obtain the frequency band for directive radiation.

1. INTRODUCTION

Electromagnetic bandgap (EBG) materials [1, 2] are periodic structures composed of dielectric and/or metallic elements. They have been the subject of intensive research in the past few years in solid state physics, optics, and microwave domains, because of their potentialities to control the propagation of electromagnetic waves. An important feature of these structures is their ability to open a bandgap that is a frequency range for which the propagation of electromagnetic waves is forbidden whatever the direction of propagation and the polarization. They are also characterized by the ability to open localized electromagnetic modes inside the forbidden frequency bandgap by introducing defects into the periodical structures. Several potential applications have been suggested for EBG materials in microwave and antenna domains, such as suppressing

surface waves [3], designing single-feed compact high-gain antennas [4, 5] or creating controllable beams [6, 7].

Recently, new periodic structures, Cylindrical Electromagnetic Band Gap (CEBG) structures, have been introduced and used as models to develop new directive antennas or new beam switching antennas [8–10]. To obtain the beam switching, the proposed technique consists of creating defects with discontinuous wires in an initial continuous wires structure, in order to obtain a directive beam turning on 360° . The proposed systems allows to avoid the inconvenience of deterioration of mechanically steering systems and reduces also the complexity and the cost by comparison with adaptive antenna arrays [12] or phased arrays [13]. However, the focusing characteristics of CEBG structures composed of metallic wires and with defects have not been studied enough. The frequency of maximum directivity, the limit frequency and the optima structures have to be determined.

The objective of this paper is to present a theoretical study of these CEBG structures, with defects, for directive antennas application. Numerical simulations were carried out to calculate the radiation patterns of these structures, at different frequencies, using the Finite Difference Time Domain (FDTD) method, where a line source is used for the excitation and the CEBG structures are considered infinite in the vertical direction. The effect of the number of cylindrical layers and the effects of the positions of the defects are studied. From these results, the structures giving the maximum of directivity are determined. Furthermore, the transmission coefficient of the cylindrical periodic structures without defect is used to determine the limit frequency for obtaining a structure with a directive pattern.

In Section 2, the focusing characteristics of CEBG structures is analyzed for different defect configurations, and the structure giving the best focusing characteristics and the limit frequency for directive radiation are determined from the numerical results. The defects consists of removing one or multiple wires. Then, in Section 3, the effects of the number of layers in the radiation patterns are studied. The near field distribution is also analyzed in order to have better understanding of the behavior of these structures.

2. CEBG STRUCTURES WITH DIFFERENT DEFECT CONFIGURATIONS

It is well known that introducing imperfections, which are also called defects, into a periodic structure, can produce localized modes within the bandgap. In this section, different defect configurations are introduced in a cylindrical EBG structure. The effect of the defect

configurations in the focusing characteristics of CEBG structures with metallic wires are analyzed.

The simulations were carried out with the FDTD method. The excitation is an infinite line current source and the wires are modeled using Holland *et al.* thin wires formalism [13]. Electric walls are used in the vertical direction.

In Subsection 2.1, the structure composed of one layer of cylindrical periodic surface is analyzed, whereas in Subsection 2.2, the structure with three layers is studied.

2.1. Structure with One Layer

The cylindrical periodic structure composed of infinite long metallic wires shown in Fig. 3 is considered. The parameters of this structure are the diameter of the wires a , the radius C , and the angular period P_θ . We also denote by P_t ($P_t = P_\theta C$) the transversal period and by N ($N = 360/P_\theta$) the number of wires.

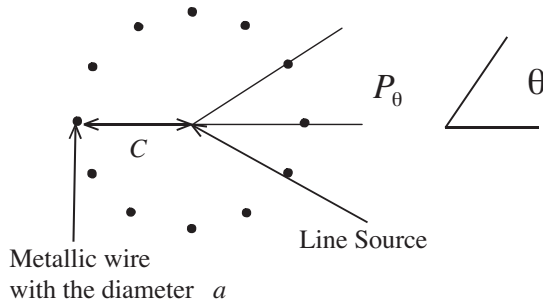


Figure 1. Periodic cylindrical structure made of infinite long metallic wires and illuminated by a line source in its center.

The structure is illuminated by an infinite line source located in the center, with a TM cylindrical wave. The structure with the following parameters is considered: $a = 2$ mm, $C = 40$ mm, and $N = 12$.

When no defect is applied to the periodic structure, one can show, after numerical studies, that the radiation pattern is omnidirectional if the condition $P_t/\lambda < 0,5$ is verified. Thus, when this condition is verified, one can define a transmission coefficient T_1 outside the cavity which considers the multiple cylindrical waves reflections between the cylindrical surface and the center. T_1 is defined as the radiated transverse electric field outside the cavity normalized by the radiated field of the source with the cylindrical surface not present.

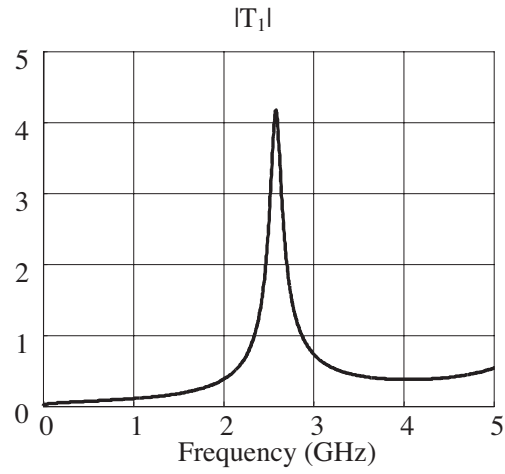


Figure 2. Radiated field outside the cavity normalized by the incident field ($|T_1|$).

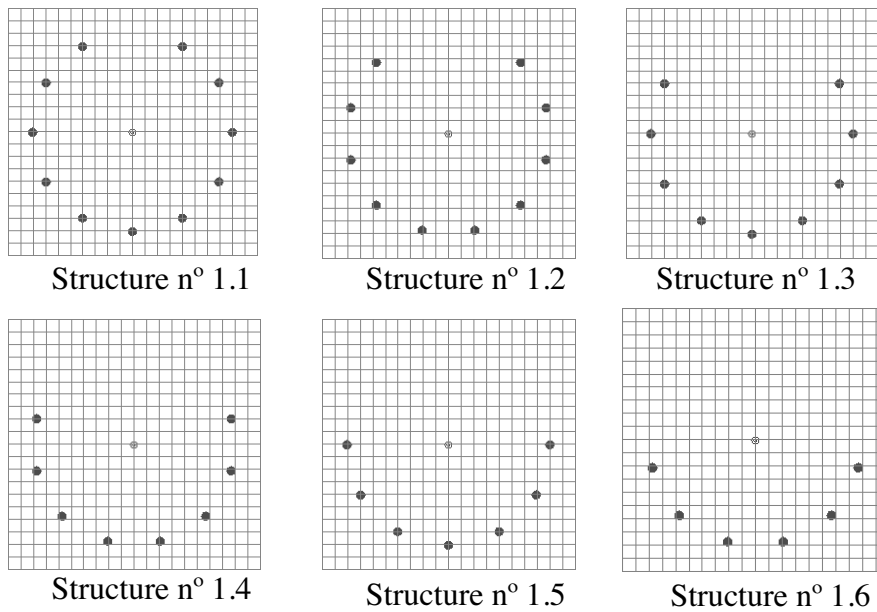


Figure 3. Different configurations of the cylindrical structures with one layer and with defects (view in the FDTD model).

This coefficient is plotted in Fig. 2 by using the semi-analytical method proposed in [10].

From Fig. 2, a resonance occurs at 2.58 GHz for the coefficient T_1 .

In order to modify the radiation pattern of the structure of Fig. 1, different structures, where one or multiple wires are removed in the initial cylindrical structure, as illustrated in Fig. 3 are considered. For these six cases the radiation patterns have been computed for different frequencies included in the band 0 GHz–5 GHz. After numerical studies, for frequencies lower than 3.5 GHz, the radiation patterns present a main beam in the direction of the defects ($\theta = 90^\circ$). For frequencies higher than 3.5 GHz, the side lobes become more dominant or the maximum of radiation is no longer at $\theta = 90^\circ$. Thus, only frequencies lower than 3.5 GHz are considered. For the different configurations presented in Fig. 3, the half power beamwidth ($\Delta\theta_{3\text{dB}}$) of the main beam and the side lobes level (or the back radiation level when there is no side lobes) are plotted vs. frequency in Figs. 4 and 5, respectively.

From Fig. 4, one can see that Structure $n^\circ 1.4$ presents the minimum half-power beamwidth for all frequencies, whereas Structure $n^\circ 1.1$ is the least directive structure. From Fig. 5, it can be seen that Structure $n^\circ 1.6$ presents the lowest side lobes level near the resonant

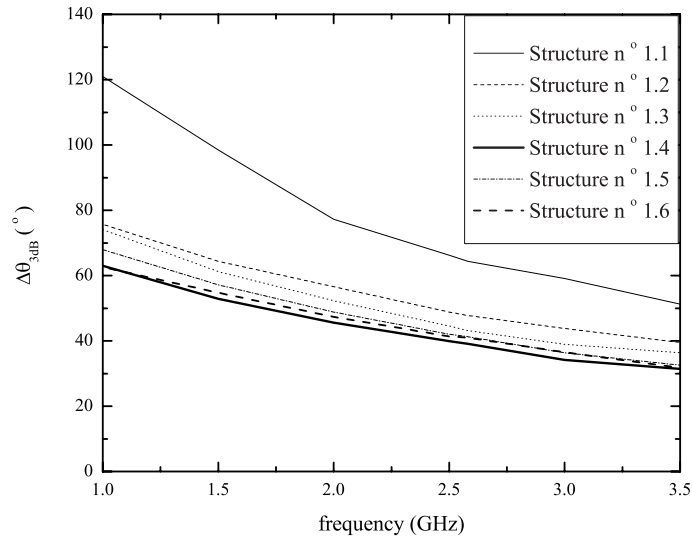


Figure 4. Half power beamwidth of the main beam vs. frequency for the different configurations in Fig. 3.

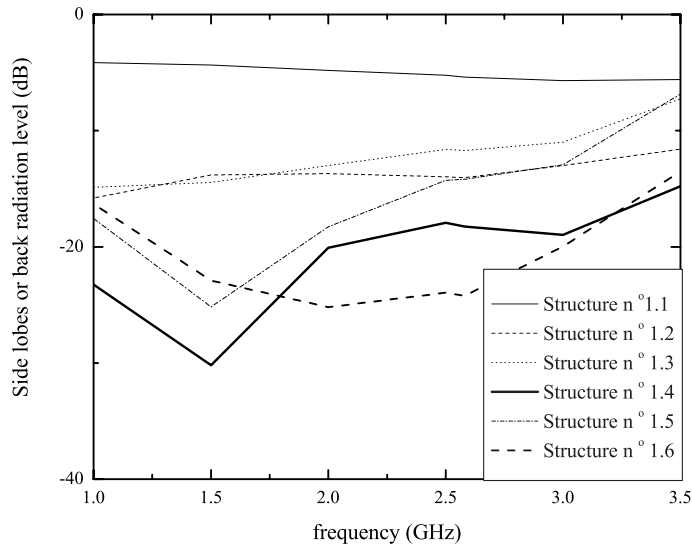


Figure 5. Side lobes or back radiation level vs. frequency for the different configurations in Fig. 3.

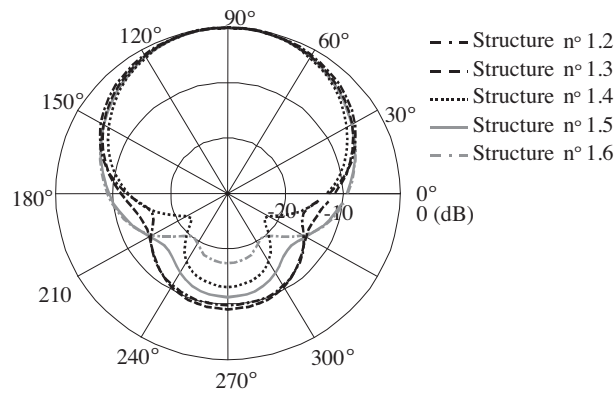


Figure 6. Radiation pattern at 2.58 GHz for the different structures in Fig. 3.

frequency of the coefficient T_1 (2.58 GHz).

Figure 6 shows the radiation patterns of the different structures at the resonant frequency of T_1 , 2.58, GHz (the radiation pattern of Structure n° 1.1 is not presenting, as it is not sufficiently directive).

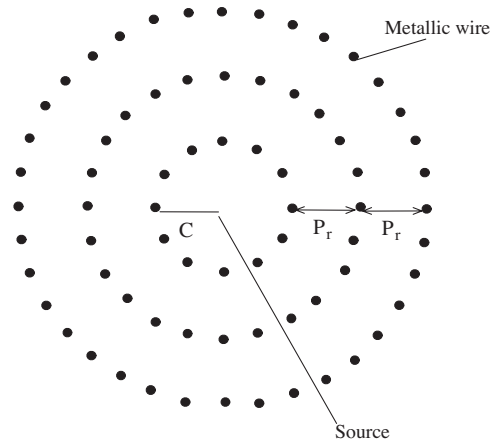


Figure 7. Cylindrical periodic structure with three layers.

2.2. Structure with Three Layers

Now, we consider the cylindrical periodic structure composed of three layers as illustrated in Fig. 7.

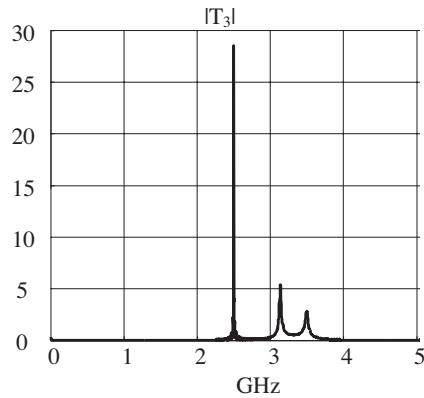


Figure 8. Coefficient $|T_3|$ for the three layers structure with the following parameters : $C = Pr = 40$ mm, $P\theta_1 = \pi/6$, $a = 2$ mm.

All the layers have the same transversal period (P_t), and the distance between the layers is called P_r (radial period). The following parameters are considered : $C = Pr = 40$ mm, $P\theta_1 = \pi/6$, $a = 2$ mm.

Using a semi-analytical method based on a cascading approach

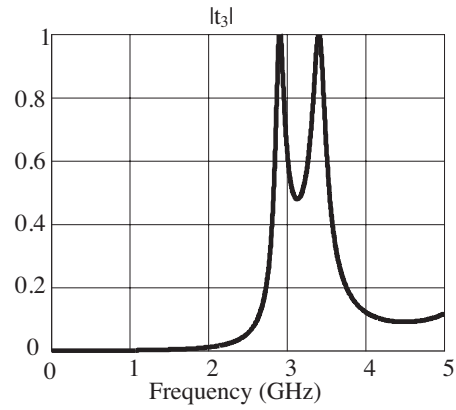


Figure 9. Coefficient $|t_3|$ for the three layers structure with the following parameters $C = Pr = 40$ mm, $P\theta_1 = \pi/6$, $a = 2$ mm.

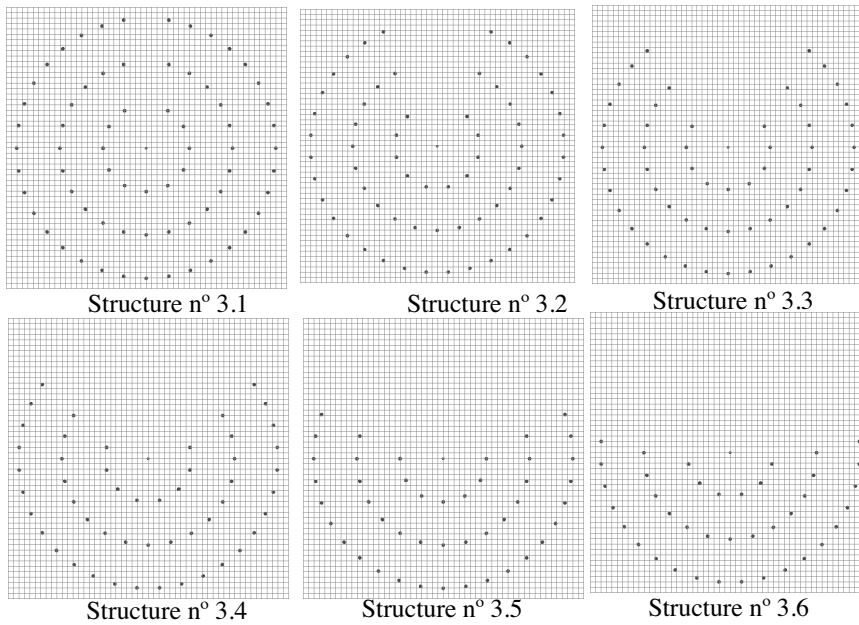


Figure 10. Different configuration of the cylindrical structure with three layers and with defects (view in the FDTD model).

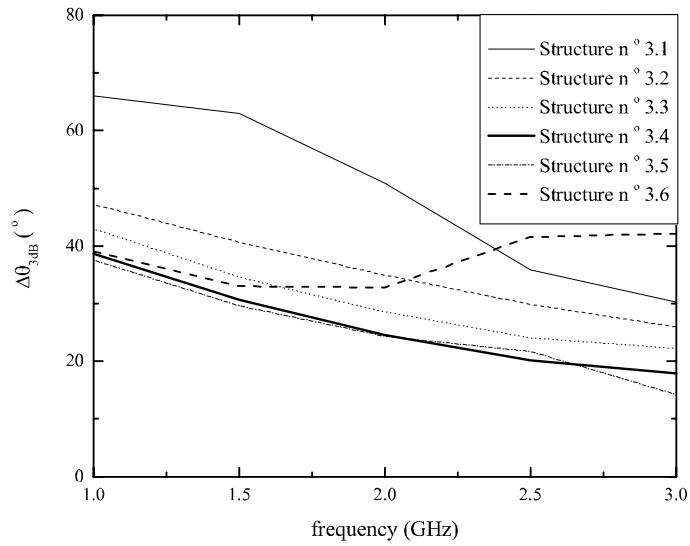


Figure 11. Half power beamwidth of the main beam vs. frequency for the different configurations in Fig. 15.

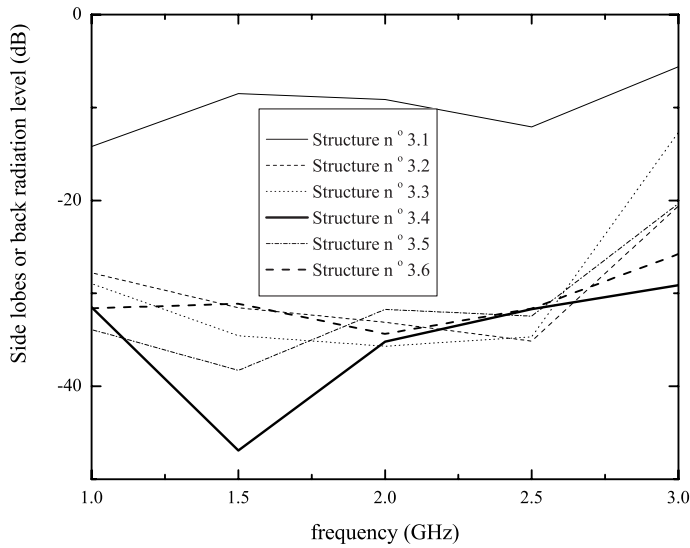


Figure 12. Side lobes or back radiation level vs. frequency for the different configurations in Fig. 15.

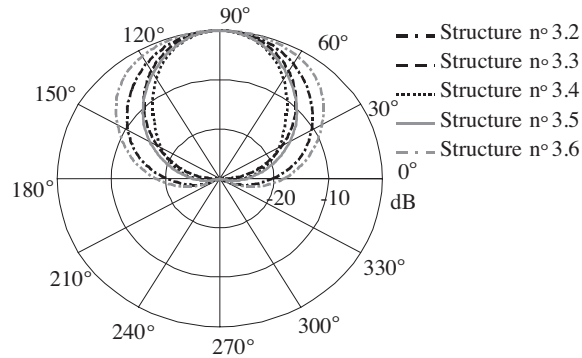


Figure 13. Radiation pattern at 2.5 GHz for the different structures in Fig. 15.

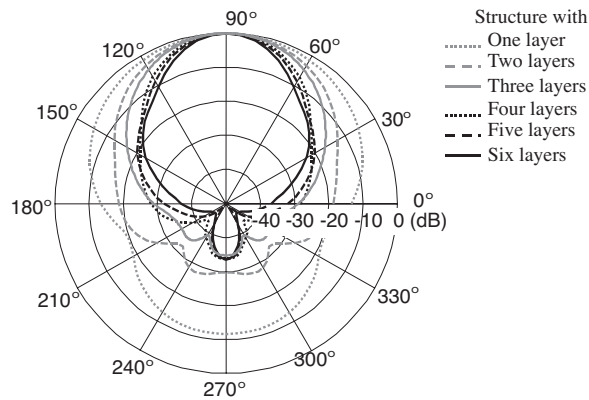


Figure 14. Radiation patterns of the structures with defects at 2.5 GHz for different number of layers.

[10], the coefficients $|T_3|$ and $|t_3|$ for the structure of Fig. 7 have been computed and are reported in Figs. 8 and 9, respectively. The coefficient $|T_3|$ is the response of the structure considering the multiple reflection with the center, whereas the coefficient $|t_3|$ is the response of the structure if the multiple reflections with the center are not considered [10].

From Figs. 8 and 9, the first resonance for $|T_3|$ occurs at 2.5 GHz, whereas the resonance for $|t_3|$ occurs at 2.9 GHz.

The structures with different configurations of defects described in Fig. 10 were analyzed. The defects are applied in the following way:

when n wires are removed in the first layer, $2n - 1$ are removed in the second layer and $3n - 2$ are removed in the third one (for $n = 1$ to 6). For frequencies lower than 3 GHz, the radiation patterns present a main beam in the direction of the defects ($\theta = 90^\circ$). For higher frequencies, the side lobes become more dominant or the maximum of radiation is not at $\theta = 90^\circ$. Thus, only frequencies lower than 3 GHz are considered.

It is interesting to note that the limit frequency correspond to the first resonant frequency of the coefficient $|t_3|$ (which does not consider the multiple reflection with the center) and not to the first frequency of $|T_3|$. This observation has been verified with structures with other number of layers. This is certainly due to the fact that when defects are applied to the structure the multiple reflections with the center became negligible. Furthermore, in the pass-band of $|t_3|$, the structure is not directive, because a major part of the energy pass through the part of the structure without defects.

For the different configurations presented in Fig. 10, the half power beamwidth ($\Delta\theta_{3\text{dB}}$) of the main beam and the side lobes level (or the back radiation level when there is no side lobes) are plotted *vs.* frequency in Figs. 11 and 12, respectively. From Fig. 11, one can see that Structures $n^\circ 3.4$ and $n^\circ 3.5$ present the minimum half-power beamwidth for all frequencies. From Figs. 11 and 12, Structure $n^\circ 3.1$ is the least directive. From Fig. 11, it can be seen that Structure $n^\circ 3.6$ presents the lowest side lobes level near the resonance. Structure $n^\circ 3.3$ presents a good compromise between small half-power beamwidth and low side lobes. Fig. 13 shows the radiation patterns of the different structures at the resonant frequency of the coefficient T_3 (2.5 GHz).

3. EFFECT OF THE NUMBER OF LAYERS AND DISTRIBUTION OF THE FIELD

Simulations were also done for structures with two, four, five and six cylindrical layers. The same parameters than previously have been used. The cylindrical layers have the same transversal period (P_t) and the distance between each layer is the same (P_r). In the structures with defects, we consider to remove n wires in the first layer, $2n - 1$ in the second, $3n - 2$ in the third, $4n - 3$ in the fourth and so on. The case where three wires are removed in the first layer is considered ($n = 3$).

For structures with two, four, five and six cylindrical layers, the first resonant frequencies of the transmission coefficients which consider the multiple reflection with the center are also near 2.5 GHz. Fig. 14 presents the computed radiation patterns of the different structures at 2.5 GHz.

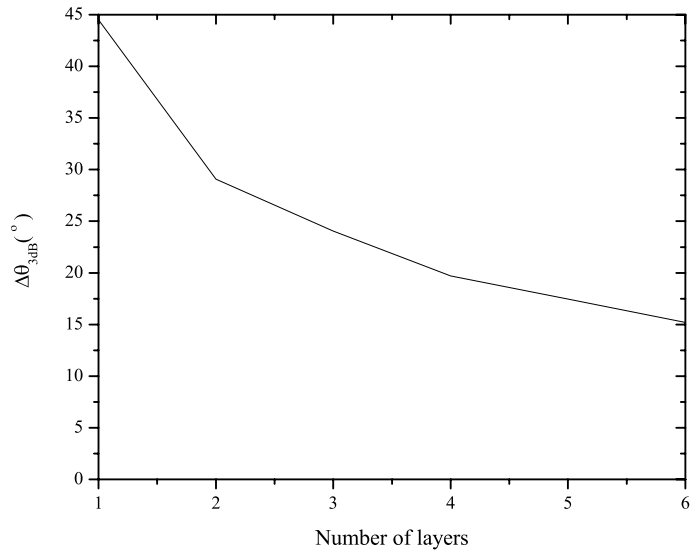


Figure 15. Half power beamwidth of the main beam at 2.5 GHz vs. the number of layers (three wires are removed in the first layer).

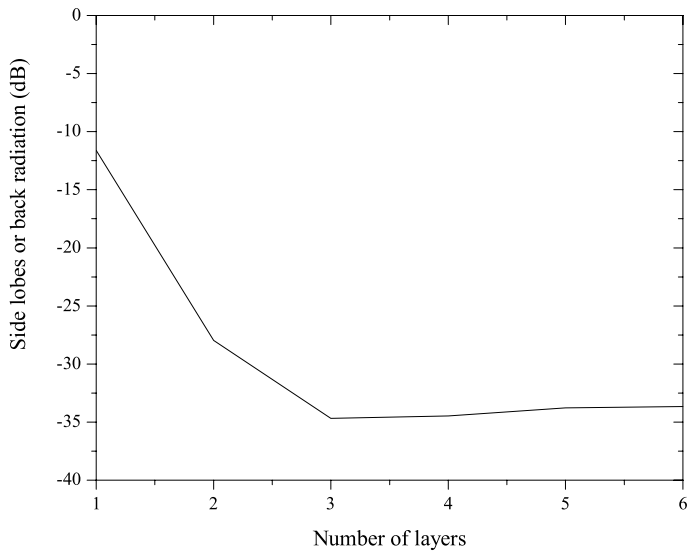


Figure 16. Side lobes or back radiation level at 2.5 GHz vs. the number of layers (three wires are removed in the first layer).

From this figure, the directivity increases when the number of layers increases. Figures 15 and 16 show the half power beamwidth ($\Delta\theta_{3\text{ dB}}$) of the main beam and the side lobes level (or the back radiation level when there is no side lobes), respectively, *vs.* frequency.

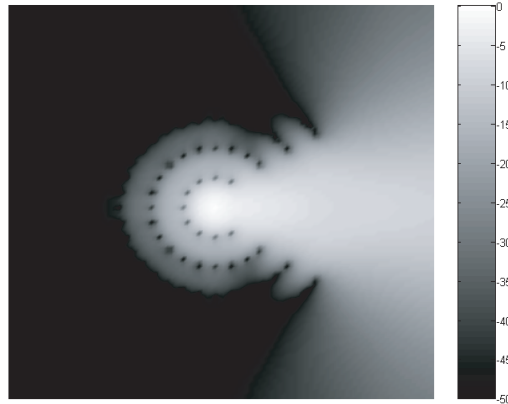


Figure 17. Distribution of the transverse electric field at 2.5 GHz (in dB) in the structure with four layers and with defect (three wires are removed in the first layer).

The decrease of the half-power beamwidth when the number of layer increases can be explained by the widening of the radiating aperture, and the decrease of the side lobes level is due to the decrease of the stop-band (band-gap) level in the response of the CEBG structure. A significant improvement of the beamwidth and the front to back ratio is obtained when the number of layers goes from 1 to 2. a smaller improvement is obtained when another element is added. With further inclusions of layers, there are no significant improvements.

Figs. 17 and 18 show the distributions of the transverse electric field in the structures with four and six layers, respectively, at 2.5 GHz. From these figures, the most part of the energy is concentrated in the three first layers. Then, increasing the number of layers is not very useful. This is an explanation of the small difference between the radiation performance of the structure with three layers and the structures with more layers.

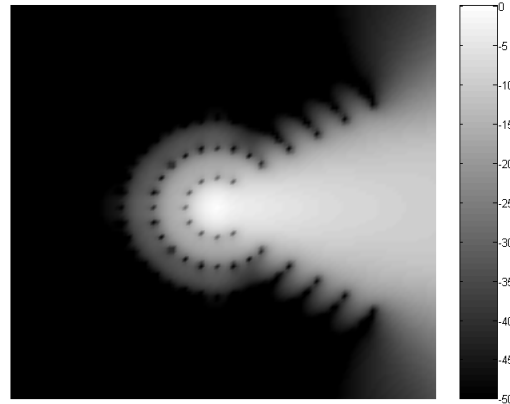


Figure 18. Distribution of the transverse electric field at 2.5 GHz (in dB) in the structure with six layers and with defect (three wires are removed in the first layer).

4. CONCLUSION

A numerical analysis of the radiation characteristics of cylindrical Electromagnetic Band Gap (EBG) structures constituted of metallic wires and with defects has been presented. The simulations were carried out with a rigorous full-wave method, where the excitation is a line source and the CEBG structure is considered infinite in the vertical direction. An important result of the proposed analysis is that the frequency band where the structures present a directive beam can be determined thanks to the response of the structures without defect, and if the multiple reflections with the center are not considered. The directivity depends on the defect configuration and it increases when the number of cylindrical layers increases. In addition, the repartition of the field in these structures has been presented and discussed. Thanks to their circular symmetry, cylindrical Electromagnetic Band Gap structures have potential application for designing antennas with a reconfigurable directive beam over 360° range.

REFERENCES

1. Joannopoulos, J., R. D. Meade, and J. N. Winn, *Photonic Crystals: Molding the flow of light*, Princeton University Press, Princeton, NJ, 1995.

2. Yablonovitch, E., "Inhibited spontaneous emission in solid state physics," *Phys. Rev. Lett.*, Vol. 58, 2059–2062, May 1987.
3. Yang, F. and Y. Rahmat-Samii, "Microstrip antennas integrated with electromagnetic bandgap (EBG) structures: a low mutual coupling design for array applications," *IEEE Trans. Antennas Propag.*, Vol. 51, 2936–2946, Oct. 2003.
4. Thevenot, M., C. Cheype, A. Reineix, and B. Jecko, "Directive photonic band-gap antennas," *IEEE Trans. Microwave Theory Tech.*, Vol. 47, 2115–2122, Nov. 1999.
5. Boutayeb, H. and T. A. Denidni, "Analysis and design of a high-gain antenna based on a metallic crystal," *Journal of Electromagnetic Wave and Application*, Vol. 20, 599–614, 2006.
6. Lourtioz, J. M., A. De Lustrac, F. Gadot, S. Rowson, A. Chelnokov, T. Brillat, A. Ammouche, J. Danglot, O. Vanbesien, and D. Lippens, "Toward controllable photonic crystals for centimeter and millimeter wave devices," *J. Lightwave Tech.*, Vol. 17, 2025–2031, Nov. 1999.
7. Poilasne, G., P. Pouliquen, K. Mahdjoubi, L. Desclos, and C. Terret, "Active metallic photonic bandgap material MPBG: experimental results on beam shaper," *IEEE Trans. Antennas Propag.*, Vol. 48, 117–119, Jan. 2000.
8. Boutayeb, H., K. Mahdjoubi, and A. C. Tarot, "Analysis of radius-periodic cylindrical structures," *Proc. IEEE AP-S Int. Symp. Dig.*, Vol. 2, 813–816, 2003.
9. Ratasjack, P., T. Brillat, F. Gadot, P. Y. Garel, A. de Lustrac, H. Boutayeb, K. Mahdjoubi, A. C. Tarot, and J. P. Daniel, "A reconfigurable EBG structure for a beam steering base station antenna," *JINA, Journee Internationales de Nice sur les Antennes*, November 2004.
10. Boutayeb, H., T. A. Denidni, K. Mahdjoubi, A.-C. Tarot, A. Sebak, and L. Talbi, "Analysis and design of a cylindrical EBG based directive antenna," *IEEE Trans. Antenna and Propagation*, Vol. 54, 211–219, Jan. 2006.
11. Compton, R. T., Jr., *Adaptive Antennas: Concepts and Performance*, Prentice-Hall, Englewood Cliffs, NJ, 1988.
12. Mailloux, R. J., *Phased Array Antenna Handbook*, Artech House, Boston, MA, 1994.
13. Holland, H. and L. Simpson "Finite-difference analysis of EMP coupling to thin struts and wires," *IEEE Trans. Electromagn. Compat.*, Vol. 23, 88–97, May 1981.